

# A new double-foil soft x-ray array to measure $T_e$ on the MST reversed field pinch<sup>a)</sup>

M. B. McGarry,<sup>1,b)</sup> P. Franz,<sup>2</sup> D. J. Den Hartog,<sup>1</sup> and J. A. Goetz<sup>1</sup>

<sup>1</sup>*Department of Physics, University of Wisconsin-Madison, Madison, Wisconsin 53706, USA*

<sup>2</sup>*Consorzio RFX, Associazione Euratom-ENEA per la Fusione, 35127 Padova, Italy*

(Presented 20 May 2010; received 16 May 2010; accepted 10 July 2010; published online 8 October 2010)

A soft x-ray (SXR) diagnostic to measure electron temperature on the Madison Symmetric Torus using two complementary methods is presented. Both methods are based on the double-foil technique, which calculates electron temperature via the ratio of SXR bremsstrahlung emission from the plasma in two different energy ranges. The tomographic emissivity method applies the double-foil technique to a tomographic reconstruction of SXR emissivity, creating a two-dimensional map of temperature throughout the plasma. In contrast, the direct brightness method applies the double-foil technique directly to the measured brightness and generates vertical and horizontal radial profiles. Extensive modeling demonstrates advantages and limitations in both techniques. For example, although the emissivity technique provides a two-dimensional mapping of temperature, its reliance on multiple tomographic inversions introduces some artifacts into the results. On the other hand, the more direct brightness technique avoids these artifacts but is only able to provide a radial profile of electron temperature. © 2010 American Institute of Physics. [doi:10.1063/1.3481167]

## I. INTRODUCTION

Soft x-ray (SXR) bremsstrahlung brightness data have been tomographically reconstructed to give measurements of emissivity for some time.<sup>1</sup> SXR tomography diagnostics typically have fast time response (10 s of kHz), allowing the study of plasma structure dynamics. For example, two-dimensional emissivity maps have been created on the MST and RFX reversed field pinch experiments to study the evolution of magnetic islands.<sup>2,3</sup> Moreover, the double-foil ratio technique can be applied to brightness or emissivity measurements to calculate electron temperature ( $T_e$ ). The double-foil technique has been used on RFX and NSTX to give single-point and radial profile measurements of  $T_e$ .<sup>4,5</sup> Initial  $T_e$  measurements have also been made in two-dimensions (2D) on MST from tomographically reconstructed emissivity maps.<sup>6</sup>

However, application of the double-foil technique to 2D emissivities on MST has exposed some issues unique to the construction of MST. For example, the presence of impurity radiation due to the aluminum vessel walls necessitates the use of beryllium filters thicker than  $\sim 200 \mu\text{m}$  to make SXR bremsstrahlung brightness measurements. This reduces the overall SXR signal level and makes the double-foil technique extremely sensitive to small variations in emissivity. As a result, artifacts are introduced into the tomographic temperature profile that may mimic  $T_e$  islands.

This paper describes an upgrade to the SXR tomography

diagnostic on MST that will for the first time enable two complementary applications of the double-foil technique to determine electron temperature simultaneously. A new geometry that expands edge coverage of the plasma will improve the two-dimensional  $T_e$  measurements using tomographic reconstructions. At the same time, multiple beryllium filter thicknesses on shared lines-of-sight will result in a radial profile of  $T_e$  when the double-foil technique is applied directly to SXR brightness.

## II. METHODOLOGY

The double-foil technique calculates electron temperature by taking the ratio of SXR signals through two different filters coming from a single location in the plasma.<sup>7</sup> The measured SXR emissivity  $\varepsilon$  and brightness  $f$ , along the line-of-sight  $L$ , due to bremsstrahlung radiation in the plasma are given by

$$\varepsilon = K \int_E dEA(E)T(E, Be) \left\{ \frac{n_e^2(r)}{\sqrt{T_e(r)}} \exp\left[-\frac{E}{T_e(r)}\right] \right\}, \quad (1)$$

$$f(L) = \int_L dL\varepsilon. \quad (2)$$

In these equations, for a given energy  $E$ ,  $K$  is a constant,  $A(E)$  is the absorption function of the detector, and  $T(E, Be)$  is the transmission function of a beryllium filter with thickness  $Be$ .  $n_e$  and  $T_e$  are the electron density and temperature, respectively. It follows that the ratio of the emissivities or brightnesses from the same part of the plasma through two different beryllium filter thicknesses are each a function of the electron temperature in that region.<sup>8</sup> The precise relation

<sup>a)</sup> Contributed paper, published as part of the Proceedings of the 18th Topical Conference on High-Temperature Plasma Diagnostics, Wildwood, New Jersey, May 2010.

<sup>b)</sup> Electronic mail: mbmcgarry@wisc.edu.

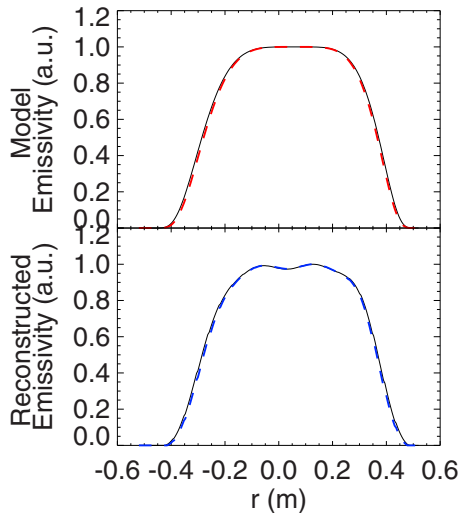


FIG. 1. (Color online) Top—normalized model emissivity profiles for two Be filters, where the dashed line is a foil with twice the thickness of the solid line, have nearly identical shapes. Bottom—the reconstructed emissivity profiles after the model brightness has been tomographically inverted show small oscillations in the core region of the plasma.

between the ratio and the temperature is a polynomial function whose coefficients can be found by modeling the bremsstrahlung radiation for many plasma temperatures.<sup>3,7</sup>

Simulations explore the temperature measuring capabilities of the diagnostic upgrade using both the direct brightness and tomographic emissivity techniques. Simulated emissivity due to bremsstrahlung radiation from a model plasma with a characteristic profile  $T_e(r)$  is combined with the diagnostic geometry to create a model brightness profile. The direct brightness technique applies the ratio to the simulated brightness, resulting in a radial profile of  $T_e$ . Because temperature is not a line-integrated quantity, an inversion cannot be done to determine contributions from individual regions of the plasma, rather the measurement gives the hottest  $T_e$  along each line-of-sight. The two-dimensional emissivity [ $\epsilon(r, \theta)$ ] is obtained by tomographic inversion of the model brightness. The tomographic  $T_e$  is then found by applying the ratio technique to this reconstructed emissivity, which results in a two-dimensional map of  $T_e$ . The results from both  $T_e$  calculations are compared with the input  $T_e(r)$  profile.

### III. LIMITATIONS OF TOMOGRAPHICALLY RECONSTRUCTED $T_e$ ON MST

Figure 1 (top) shows normalized model emissivity profiles for a “thin” (408  $\mu\text{m}$ , solid line) and a “thick” (821  $\mu\text{m}$ , dashed line) Be filter. Despite the difference in the energy regimes being accessed by the two filters, the shapes of the curves are nearly identical. In the plasma regime accessed by MST ( $T_e \sim 1\text{--}2$  keV), the ratio  $R$  between the two emissivity curves is extremely flat. As a result, very small changes in  $R$  lead to large apparent changes in tomographic  $T_e$ . This causes small deviations from the ideal emissivity to be amplified in the final  $T_e$  measurement. Figure 1 (bottom) shows the reconstructed emissivity for this same simulation, with oscillations of  $\sim 5\%$  due to a mathematical instability related to probe geometry. Figure 2 shows the calculated

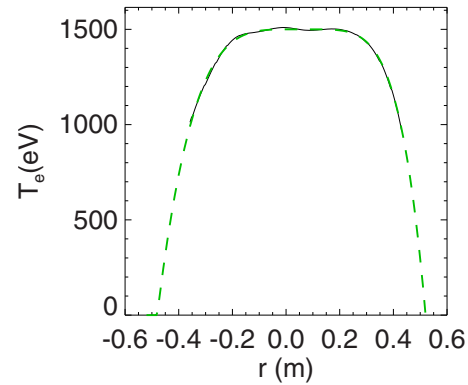


FIG. 2. (Color online) Calculated tomographic  $T_e$  from the emissivity ratio (solid) compared to the profile input into the simulation (dashed).

temperature profile for this simulation. Although in this case the artifacts in  $T_e$  are small, further analysis has shown that when a Gaussian distribution of noise with an amplitude of 5% is added to the simulation, oscillations in the resulting  $T_e$  calculation become as large as 20%. Magnetic structures are expected to produce  $T_e$  islands with  $\sim 10\%$ – $20\%$  of the equilibrium temperature, so this artifact is a serious concern.

### IV. DIAGNOSTIC UPGRADE

The original SXR tomography diagnostic was comprised of two pairs of SXR probes at a single toroidal location, where each pair had a  $90^\circ$  poloidal separation between the two probes.<sup>9</sup> The two probes using thin Be filters did not share lines-of-sight with the thick Be filter probes, so  $T_e$  could only be calculated using tomographic reconstruction, and artifacts in the profile were a persistent issue. If the two different filters had the same line-of-sight, however, a temperature calculation could be made directly from the brightness measurement,<sup>7</sup> thereby avoiding the tomographic inversion and its attendant artifacts altogether.

The diagnostic upgrade on MST, shown in Fig. 3, has two significant improvements over the previous generation. The new diagnostic is comprised of four units at separate poloidal angles, all utilizing 2 inch diameter portholes at a single toroidal location. Two probes have parallel central chords, located near the vertical axis of the plasma, while the

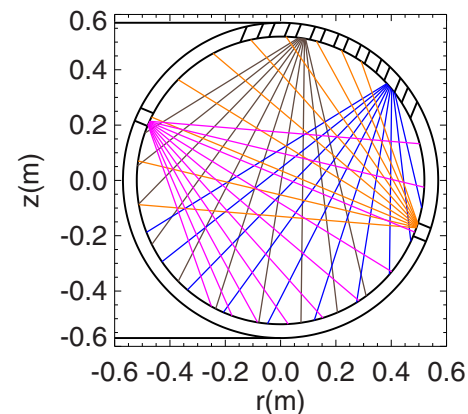


FIG. 3. (Color online) Geometry of the diagnostic upgrade, showing the ten lines-of-sight shared by 20 diodes in each probe.

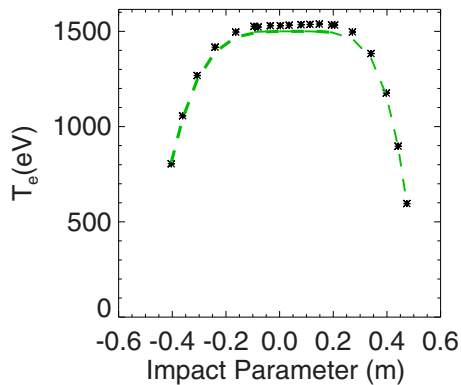


FIG. 4. (Color online)  $T_e$  calculated from the direct-brightness ratio (stars) accurately reproduces the profile input into the simulation (dashed line).

other two are  $90^\circ$  away in opposite directions. Each unit has ten lines-of-sight, and each line-of-sight is now associated with two individual silicon photodiodes (the AXUV-1ELM from IRD) looking through Be foils of different thicknesses. The shared lines-of-sight allow  $T_e$  to be calculated directly from brightness. This approximately gives the hottest temperature along each line-of-sight, resulting in near-horizontal and near-vertical radial profiles of electron temperature. Additionally, the 20 near-vertical and 20 near-horizontal measurements for each foil thickness can still be reconstructed into a two-dimensional map of tomographic  $T_e$ . The geometry of the probes has been altered to improve coverage at the edge of the plasma, which has been shown in simulations to reduce oscillations in the reconstructed emissivity and to dramatically improve the resulting tomographic  $T_e$  calculation.

Figure 4 shows the horizontal electron temperature profile as calculated by applying the double-foil technique directly to brightness in a simulated plasma. The dashed line is the temperature profile, as a function of impact parameter, used to simulate SXR emission. The stars are the temperatures calculated for each line-of-sight from the direct-

brightness ratio. The slight offset ( $\sim 5\%$ ) between the calculated and simulated temperature is believed to be due to the coefficients that define the ratio  $R(T_e)$ , and is being investigated further.

An upgraded diagnostic has been designed that improves tomographic reconstructions and reduces resulting oscillations in the electron temperature calculation by optimizing probe field-of-view. The capability to apply the double-foil technique directly to brightness measurements has been added. The electron temperature will be measured both through emissivity as a 2D tomographic reconstruction and directly through line-integrated brightness as a radial profile. Combining the data from the two techniques should help to discern true temperature structures from mathematical artifacts and noise. Results from both techniques will be verified with a Thomson scattering diagnostic. The excellent time resolution of the SXR diagnostic will eventually enable the study of temperature structure dynamics.

<sup>1</sup>R. S. Granetz and P. Smeulders, *Nucl. Fusion* **28**, 457 (1988).

<sup>2</sup>P. Franz, L. Marrelli, P. Piovesan, I. Predebon, F. Bonomo, L. Frassinetti, P. Martin, G. Spizzo, B. E. Chapman, D. Craig, and J. S. Sarff, *Phys. Plasmas* **13**, 012510 (2006).

<sup>3</sup>P. Franz, L. Marrelli, A. Murari, G. Spizzo, and P. Martin, *Nucl. Fusion* **41**, 695 (2001).

<sup>4</sup>A. Murari, P. Franz, L. Zabeo, R. Bartiromo, L. Carraro, G. Gadani, L. Marrelli, P. Martin, R. Pasqualotto, and M. Valisa, *Rev. Sci. Instrum.* **70**, 581 (1999).

<sup>5</sup>L. F. Delgado-Aparicio, D. Stutman, K. Tritz, M. Finkenthal, R. Bell, J. Hosea, R. Kaita, B. LeBlanc, L. Roquemore, and J. R. Wilson, *J. Appl. Phys.* **102**, 073304 (2007).

<sup>6</sup>P. Franz, F. Bonomo, L. Marrelli, P. Martin, P. Piovesan, G. Spizzo, B. E. Chapman, D. Craig, D. J. Den Hartog, J. A. Goetz, R. O'Connell, S. C. Prager, M. Reyfman, and J. S. Sarff, *Rev. Sci. Instrum.* **77**, 10F318 (2006).

<sup>7</sup>T. P. Donaldson, *Plasma Phys.* **20**, 1279 (1978).

<sup>8</sup>F. C. Jahoda, E. M. Little, W. E. Quinn, G. A. Sawyer, and T. F. Stratton, *Phys. Rev.* **119**, 843 (1960).

<sup>9</sup>P. Franz, F. Bonomo, G. Gadani, L. Marrelli, P. Martin, P. Piovesan, G. Spizzo, B. E. Chapman, and M. Reyfman, *Rev. Sci. Instrum.* **75**, 4013 (2004).